Activation of JNK3α1 Requires both MKK4 and MKK7: Kinetic Characterization of in Vitro Phosphorylated JNK3α1

JeanMarie Lisnock,[‡] Patrick Griffin,[‡] Jimmy Calaycay,[‡] Betsy Frantz,[§] Janey Parsons,[§] Stephen J. O'Keefe,[§] and Philip LoGrasso*,[‡]

Departments of Molecular Design and Diversity, and Immunology and Rheumatology, Merck Research Laboratories, P.O. Box 2000, Rahway, New Jersey 07065

Received October 18, 1999; Revised Manuscript Received December 27, 1999

ABSTRACT: JNK3α1 is predominantly a neuronal specific MAP kinase that is believed to require, like all MAP kinases, both threonine and tyrosine phosphorylation for maximal enzyme activity. In this study we investigated the in vitro activation of JNK3α1 by MAP kinase kinase 4 (MKK4), MAP kinase kinase 7 (MKK7), and the combination of MKK4 + MKK7. Mass spectral analysis showed that MKK7 was capable of monophosphorylating JNK3α1 in vitro, whereas both MKK4 and MKK7 were required for bisphosphorylation and maximal enzyme activity. Measuring catalysis under V_{max} conditions showed MKK4 + MKK7-activated JNK3α1 had V_{max} 715-fold greater than nonactivated JNK3α1 and MKK7-activated JNK3α1 had V_{max} 250-fold greater than nonactivated JNK3α1. In contrast, MKK4-activated JNK3α1 had no increase in V_{max} compared to nonactivated levels and had no phosphorylation on the basis of mass spectrometry. These data suggest that MKK7 was largely responsible for JNK3α1 activation and that a single threonine phosphorylation may be all that is needed for JNK3α1 to be active. The steady-state rate constants k_{cat}, $K_{m(GST-ATF2)}$, and $K_{m(ATP)}$ for both monophosphorylated and bisphosphorylated JNK3α1 were within 2-fold between the two enzyme forms, suggesting the addition of tyrosine phosphorylation does not affect the binding of ATF2, ATP, or maximal turnover. Finally, the MAP kinase inhibitor, SB203580, had an IC_{50} value approximately 4-fold more potent on the monophosphorylated JNK3α1 compared to the bisphosphorylated JNK3α1, suggesting only a modest effect of tyrosine phosphorylation on inhibitor binding.

The c-jun NH_2-terminal kinases (JNKs)[1] are members of the mitogen-activated protein (MAP) kinase family and respond to a variety of stress-based stimuli including cytokines, osmotic shock, UV-irradiation, and hypoxia. (For recent reviews see refs *1* and *2*). The JNKs phosphorylate c-jun (*3*−*5*), ATF2 (*6*−*8*), and mitogen-activated kinase activating domain (MADD) (*9*). Three genes encode JNK, JNK1, JNK2, and JNK3, and from these, alternate splicing results in ten JNK isoforms (*6*). JNK3 is unique in that it is primarily expressed in the brain within neurons (*6*, *10*) and at low levels in heart and testis. Recently, Yang et al. (*3*) reported JNK3-deficient mice that showed reduced seizure activity and prevention of neuronal apoptosis in response to kainic acid-induced excitotoxicity. This, coupled with reports of the JNK signaling pathway being involved in neuronal apoptosis in PC-12 cells (*11*) and an inhibitor of the JNK signaling pathway that blocked motoneuron apoptosis (*12*), heightened interest in JNK as a therapeutic target for neuronal death.

For JNK1 and JNK2 to be fully active they must be phosphorylated on both threonine and tyrosine in the activation loop (TXY) found in all MAP kinases (*6*, *13*). A number of studies utilizing either targeted gene disruption of MKK4 (*14*) or immunoprecipitation of either MKK4 (*15*) or MKK7 (*16*, *17*) and subsequent activation of JNK1 or JNK2 have shown either of these upstream activators is essential for JNK activation. In a more detailed analysis, Lawler et al. (*18*) utilizing purified MKK4, MKK7, and JNK1 have shown that both MKK4 and MKK7 are needed in vitro for maximal activation of JNK1. To date, no studies have investigated the upstream activation components of JNK3.

The current study was designed to investigate the roles MKK4 and MKK7 play in the activation of JNK3α1 and to evaluate the kinetic properties of JNK3α1. Mass spectral and Western analysis were used to monitor the phosphorylation state of JNK3α1 activated by MKK4, MKK7, and MKK4 + MKK7. Steady-state kinetic analysis of the incorporation of [^{33}P]phosphate into GST-ATF2 was utilized

* To whom correspondence should be addressed. Phone: (732) 594-1271. E-mail: lograsso@merck.com.

[‡] Department of Molecular Design and Diversity.

[§] Department of Immunology of Rheumatology.

[1] Abbreviations: ATF2, activating transcription factor 2; ATP, adenosine triphosphate; BSA, bovine serum albumin; cHPLC−MS/MS, capillary high-performance liquid chromatography−tandem mass spectrometry; DTT, dithiothreitol; ECL, enhanced chemiluminescence; EDTA, ethylenediaminetetraacetic acid; ERK-2, extracellular-regulated protein kinase 2; GST, glutathione *S*-transferase; HEPES, (*N*-[2-hydroxyethyl]piperazine-*N*′-[2-ethanesulfonic acid]); IPTG, isopropyl-thio-β-D-galactoside; JNK, c-jun NH_2-terminal kinase; LC−MS, liquid chromatography−mass spectrometry; MAP, mitogen-activated protein kinase; MKK, MAP kinase kinase; MW, molecular weight; PAGE, polyacrylamide gel electrophoresis; PCR, polymerase chain reaction; PP2A, protein phosphatase 2A; PTP1B, protein tyrosine phosphatase 1B; SAPK, stress-activated protein kinase; SDS, sodium dodecyl sulfate; TBST, Tris-buffered saline−Tween.

10.1021/bi992410+ CCC: $19.00
Published on Web 02/25/2000

to determine the differences in substrate binding, inhibitor binding, and maximal turnover for bis- and monophosphorylated forms of JNK3α1.

The major findings of this study include (1) MKK4-treated JNK3α1 had minimal kinase activity in contrast to MKK7-activated JNK3α1 which was phosphorylated on threonine and had kinase activity 250-fold above basal levels, (2) MKK4 and MKK7 were required for bisphosphorylation and maximal kinase activity of JNK3α1 (715-fold higher than basal), and (3) binding of ATF2, ATP, and SB203580 and maximal turnover are largely unaffected by tyrosine phosphorylation in the activation loop.

MATERIALS AND METHODS

Cloning of JNK3α1. A DNA fragment of JNK3α1 spanning nucleotides 1−1232 was isolated from human hippocampal cDNA (Invitrogen) by PCR amplification utilizing the following two oligonucleotides:

(A) $^{5'}$CAGTCCATATGAGCCTCCATTTCTTA
TACTACTGC$^{3'}$

(B) $^{5'}$CACTAGGATCCTTACTGCTGCACCTG
TGCTGAAGGAG$^{3'}$

Oligonucleotide A contains five excess bases at the 5′ end followed by an *Nde*I restriction site, and 27 base pairs (bp) identical to those of JNK3α1. Oligonucleotide B contains five excess bases at the 5′ end followed by a *Bam*HI restriction site, a stop codon, and 23 base pairs complementary to those of JNK3α1. The JNK3α1 PCR product was subcloned into pCR2.1 (Invitrogen). An N-terminal truncated JNK3α1 spanning nucleotides 115−1232, beginning at amino acid 39 and having an alanine inserted between amino acids 39 and 40, and ending at amino acid 422 was PCR amplified from the pCR2.1 JNK3α1 vector utilizing oligonucleotides C (below) and B (above).

(C) $^{5'}$CAGTCCCATGGCTAGCAAAAGCAAA
GTTGACAACCAG$^{3'}$

Oligonucleotide C contains five excess bases at the 5′ end followed by an *Nco*I restriction site, two bases to complete the Ala codon, and 24 base pairs identical to those of JNK3α1. The DNA sequence was confirmed to be identical to that of Gupta et al. (*6*). For protein expression, truncated JNK3α1 was subcloned into pET15b (Novagen) at the *Nco*I and *Bam*HI restriction sites.

Expression and Purification of Truncated JNK3α1. Truncated JNK3α1(amino acids 39−422) was expressed in *E. coli* strain BL21(DE3) (Novagen) under the following conditions: 8 mL of a log phase culture grown in Luria Broth (LB) (Digene) supplemented with 50 μg/mL ampicillin (Sigma) was transferred to 500 mL of the same medium and grown with shaking at 240 rpm and 30 °C. At $A_{600} = 0.8$ the culture was induced with 0.8 mM (final concentration) isopropylthio-β-D-galactoside (IPTG) (Gibco) and grown with shaking at 240 rpm and 30 °C for 2 h and harvested at 4 °C by centrifugation at 2830*g*. Cell pellets were frozen at −70 °C for subsequent purification.

Frozen pellets from a 500 mL culture were resuspended in 10 mL of lysis buffer containing 50 mM HEPES, pH 7.2, 10% glycerol, 0.1 M NaCl, 2 mM DTT, and 100 μL of protease inhibitor cocktail P 8340 (Sigma). Cells were lysed at 4 °C by passage through a French press at 20 000 psi and centrifuged at 126086*g* for 30 min at 4 °C. The supernatant was diluted 4-fold with buffer A (20 mM HEPES, pH 7.0, 10% glycerol, 2 mM DTT) and applied to a 20−22 mL HiLoad (16/10) SP-Sepharose HP (Pharmacia) cation exchange column that had been preequilibrated at 4 °C with buffer A for 2 h. The column was washed with five column volumes (100 mL) of buffer A, followed by five column volumes of buffer A containing 50 mM NaCl. The sample was eluted in 2 mL fractions at a flow rate of 1 mL/min in a 160 mL linear gradient of 50−300 mM NaCl in buffer A. The collected fractions were concentrated using a Centriplus-30 (Amicon). Coomassie Brilliant Blue R-250 (BioRad) staining of 12% SDS−PAGE Tris−glycine gels (Novex) revealed greater than 95% homogeneity. The concentration of truncated JNK3α1 was determined by amino acid analysis.

Expression and Purification of MKK4 and GST-ATF2. cDNA encoding MKK4 was generated from human brain polyA RNA (Clontech) using the GeneAmp protocol (Perkin-Elmer) with oligonucleotides designed on the basis of Genbank accession no. L36870. The cDNA was modified to encode an N-terminal FLAG epitope (Kodak) and was cloned into plasmid pRMHA-3. The new plasmid (pRM-MKK4) was cotransfected with a neomycin resistance plasmid, pS2-neo, into *Drosophila* Schneider S2 cells, and clonal selection in media supplemented with 1.5 mg/mL active G418 (Gibco) for stable transfectants was carried out. S2 cells were grown in Schneider's *Drosophila* medium (Gibco) supplemented with 10% fetal calf serum (Biocell), 50 μg/mL gentamicin (Gibco), and 2 mM glutamate (Gibco) to a density of 2×10^6 cells/mL in 1 L spinner flasks at 26 °C. Expression was induced by treating cells with 1 mM $CuSO_4$ for 4 h. To induce phosphorylation of recombinant MKK4, $CuSO_4$-induced cells were stimulated with 400 mM NaCl and 2 mM Na_3VO_4 10 min prior to harvest. Cell pellets from 2 L of cells were washed with PBS and 2 mM Na_3VO_4 and lysed in 20 mM Tris, pH 7.5, 120 mM NaCl, 1% Triton X-100, 2 mM EDTA, 20 mM NaF, 4 mM Na_3VO_4, and 2 mM Pefabloc SC (Boehringer Mannheim). Extracts were centrifuged for 10 min at 13000*g*, and MKK4 from a 30 mL lysate was immunoaffinity-purified through 2.5 mL of packed anti-FLAG M2 resin (Kodak) as previously described (*19*). GST-ATF2 was expressed and purified as previously described (*19*).

Activation of JNK3α1. JNK3α1 was activated in vitro by MKK4, MKK7, and a combination of MKK4 and MKK7 in 129 μL of a buffer containing 25 mM HEPES (Sigma), pH 7.4, 10 mM $MgCl_2$ (Sigma), 2 mM DTT (Sigma), 20 mM β-glycerophosphate (Sigma), 0.1 mM Na_3VO_4, 200 μM ATP (Sigma), 225 nM JNK3α1, and 100 nM MKK4, 100 nM GST-MKK7 (Upstate Biotechnology), or 100 nM MKK4 + 100 nM GST-MKK7. Reactions were incubated at 30 °C for 2 h. Activation times as short as 1 h and as long as 18 h showed the same amount of phosphorylation and enzyme activity as the 2 h time point. The phosphorylated JNK3α1 was diluted to the appropriate concentration and used as active JNK3α1 enzyme in either the steady-state kinetic or enzyme inhibition studies.

Phosphatase Treatment of JNK3α1. Twenty microliters of JNK3α1 samples, activated as described above with the exception of using the buffer 25 mM HEPES, pH 7.4, 10 mM $MgCl_2$, and 2 mM DTT, were treated with either 180 nM PTP1B (Upstate Biotechnology) or 200 nM PP2A (Upstate Biotechnology) at 30 °C for 15 min. Phosphatase reactions were stopped with either 5 mM (final concentration) Na_3VO_4 (Sigma) for PTP1B or 10 μg/mL okadaic acid (Sigma) for PP2A. JNK3α1 activity was assayed by slight modification to that described in the steady-state kinetic section. Final concentrations were as follows: 14 μM ATP, 1.8 μM GST-ATF2, 11 nM JNK3α1, and 1 μCi [^{33}P]ATP/reaction.

Trypsin Digestion. A 227 ng sample of JNK3α1 in buffer A was digested with 1 μg of porcine trypsin (Promega) at 37 °C for 12 h.

Mass Spectrometry. Capillary HPLC−mass spectrometric (cHPLC−MS) data were acquired on a Finnigan TSQ700 mass spectrometer (San Jose, CA) equipped with a homemade microspray ionization source. Using a pressure vessel, samples were loaded onto a reversed-phase capillary column made of 100 μm i.d. fused silica capillary, pulled on one end to ∼5 μm and packed fritless with 30 mm of 10 μm C_{18} medium (Perseptive Biosystems). The column was connected in-line to an ABI 130 HPLC gradient system equipped with a flow splitter that provided ∼500 nL of eluate/min that was fed directly into the mass spectrometer. The electrospray voltage was set at 2.5 kV. Approximately 5 pmol (227 ng) of JNK3α1 was analyzed. Capillary HPLC tandem mass spectra (cHPLC−MS/MS) of JNK3α1 tryptic peptides were recorded on a Finnigan LCQ quadrupole ion trap mass spectrometer equipped with a homemade microspray ionization source as described above. Precursor ions were isolated and fragmented by using resonance excitation with a relative collision energy of 30% and an isolation width of 3 Da. Product ion spectra were interpreted manually and by the database correlation program Sequest.

Western Analysis. Activated and nonactivated samples of JNK3α1 were resolved on 12% Tris−glycine polyacrylamide gels (Novex). Proteins were transferred for 1 h at 0.1 mA to 0.45 μm poly(vinylidene difluoride) (PVDF) membranes (Millipore) using a semidry blotting system (Pharmacia). Nonspecific protein binding was blocked with 10% BSA (Sigma) in 20 mL of 25 mM Tris−HCl, pH 7.4, 150 mM NaCl, and 0.05% Tween-20 (TBST) at 4 °C overnight. Western analysis used the following antibodies: SAPK/JNK antibody (New England Biolabs), phospho-SAPK/JNK (Thr183/Tyr185) (NEB), and anti-phosphotyrosine, clone 4G10 (Upstate Biotechnology). All primary antibodies were diluted 1:2000 in 25 mM Tris−HCl pH 7.4, 150 mM NaCl, and 0.05% Tween-20 containing 1% BSA and incubated for 1 h at 22 °C. Membranes were washed four times in 20 mL of TBST before appropriate secondary antibodies were added. Goat anti-rabbit IgG (H + L) HRP conjugate (Biorad) was diluted 1:10000 for JNK, and goat anti-mouse IgG (H + L) HRP conjugate (Pierce) was diluted 1:10000 for anti-pY and anti-pJNK detection. The secondary antibodies diluted in 20 mL of TBST containing 1% BSA were added to the membranes and incubated for 1 h at 22 °C. Membranes were washed four times in 20 mL of TBST, and the proteins were detected using 2−3 mL of chemiluminescence reagents ECL (Amersham Pharmacia Biotech). The immunoblots were exposed to X-Omat X-ray film (Kodak) for a period of 30 s to 4 min. Total JNK3α1 protein added per lane was 59 ng (1.3 pmol). The described activating enzymes were also present in the activated JNK3α1 samples at 25 ng (0.6 pmol) for MKK4 and 39 ng (0.6 pmol) for GST-MKK7. The band seen at 65 kDa represents GST-MKK7.

Steady-State Kinetics. Initial velocity studies utilized to determine the steady-state constants for ATP and GST-ATF2 were carried out in 100 μL volumes containing the final concentrations of the following: 25 mM HEPES (Sigma), pH 7.4, 10 mM $MgCl_2$ (Sigma); 2 mM DTT (Sigma), 20 mM β-glycerophosphate (Sigma), 0.1 mM Na_3VO_4 (Sigma), 2 μCi [γ-^{33}P]ATP (2000 Ci/mmol; 1 Ci = 37 GBq) (Amersham), 0.4−128 μM ATP (Pharmacia), and 0.125−2 μM GST-ATF2. The reactions were initiated with the addition of 0.45−2 nM JNK3α1 (final concentration) and incubated for 30 min at 30 °C. Under these conditions, less than 10% of substrate was converted to product and the reaction was linear over a time course up to 90 min. Reactions were stopped with 100 μL of 100 mM EDTA/15 mM sodium pyrophosphate. Immobilon-P 96-well plates (Millipore MAIPNOB 10) were pretreated with 100 μL of methanol, followed by 100 μL of 15 mM sodium pyrophosphate. Fifty microliters of the stopped reaction was spotted in triplicate on the immobilon-P 96-well plate. The samples were vacuum-filtered and washed three times each with 100 μL of 75 mM H_3PO_4 to remove unincorporated [γ-^{33}P]ATP. After the third H_3PO_4 wash and a final filtration step to remove H_3PO_4, 50 μL of Microscint-20 (Packard) was added to each well, and samples were analyzed on a Packard Topcount liquid scintillation counter. Data are from the average of two experiments each filtered in triplicate. The initial velocities as a function of both GST-ATF2 and ATP were fitted to equations for the ternary-complex (sequential) mechanism (*20*). Kinetic constants were determined from nonlinear least-squares analysis (*20*).

Enzyme Inhibition. Enzyme inhibition studies were performed at 30 °C for 30 min with 0.5 μM GST-ATF2, 1 μM ATP, 1 nM activated JNK3α1, and 30 nM to 300 μM SB203580 (CalBiochem) in the enzyme buffer described above. IC_{50} values were determined by fitting the data to the equation for a four-parameter logistic (*20*). The errors shown are standard errors. Data are from the average of three experiments filtered in triplicate.

RESULTS

Phosphorylation of JNK3α1 by MKK4, MKK7, and MKK4 + MKK7. To investigate the individual and additive/synergistic contributions MKK4 and MKK7 make toward JNK3α1 phosphorylation and activation, we utilized purified enzyme components to probe the specificity of each MAP kinase kinase toward JNK3α1 in vitro. Figure 1A presents the anti-JNK Western blot of JNK3α1 samples that were not treated (lane 4) or were treated with MKK4 (lane 1), MKK7 (lane 2), or MKK4 + MKK7 (lane 3) showing roughly equal immunoreactivity of JNK3α1 (∼44 kDa). The band at ∼64 kDa (lanes 2 and 3) is likely GST-MKK7 that cross-reacts with the anti-JNK antibody. Figure 1B shows the anti-phosphotyrosine Western blot of JNK3α1 samples

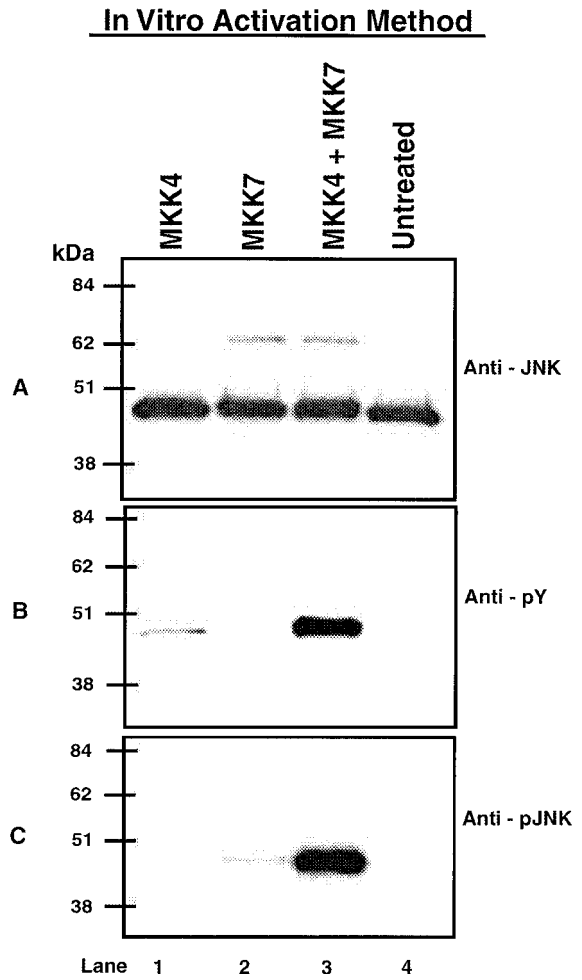

FIGURE 1: Western blot analysis of in vitro MKK-activated JNK3α1. Samples from a 12% SDS−PAGE Tris−glycine gel were transferred to PVDF membranes and detected with a horseradish peroxidase-coupled immunoassay utilizing enhanced chemiluminescence. Approximately 1.3 pmol (59 ng) of JNK3α1 was applied in all lanes. Lane 1, MKK4-treated JNK3α1; lane 2, MKK7-activated JNK3α1; lane 3, MKK4 + MKK7-activated JNK3α1; lane 4, untreated JNK3α1. Molecular mass standards (kDa) (Gibco) are shown on the left-hand side of the figure. (A) Anti-JNK blotting. (B) Anti-phosphotyrosine blotting. (C) Anti-phospho-JNK blotting.

indicating that MKK4 (lane 1) and to a much greater extent MKK4 + MKK7 (lane 3) were capable of phosphorylating JNK3α1 on tyrosine whereas MKK7 was not (lane 2). Figure 1C presents the anti-phospho-JNK Western blot of JNK3α1 samples indicating that neither MKK4- nor MKK7-treated JNK3α1 (lanes 1 and 2) was bisphosphorylated to any significant extent. However, the combination of MKK4 + MKK7 treatment (lane 3) showed a band of approximately 44 kDa that had been bisphosphorylated and was likely JNK3α1.

We were able to corroborate and extend the findings from Western analysis by cHPLC−MS (Figure 2). Figure 2A shows the mass spectrum of the non-MKK-treated reaction for JNK3α1. The experimentally determined MW of 44 070 Da was consistent with no phosphorylation and two oxidations of JNK3α1 and in line with the calculated MW for des-methionine JNK3α1 that is oxidized twice (44 064). Similarly, MKK4-treated JNK3α1 (Figure 2B) showed no phosphorylation and had a MW consistent with that of unphosphorylated des-methionine JNK3α1 that is oxidized twice. MKK7-activated JNK3α1 had a MW of 44 141 Da

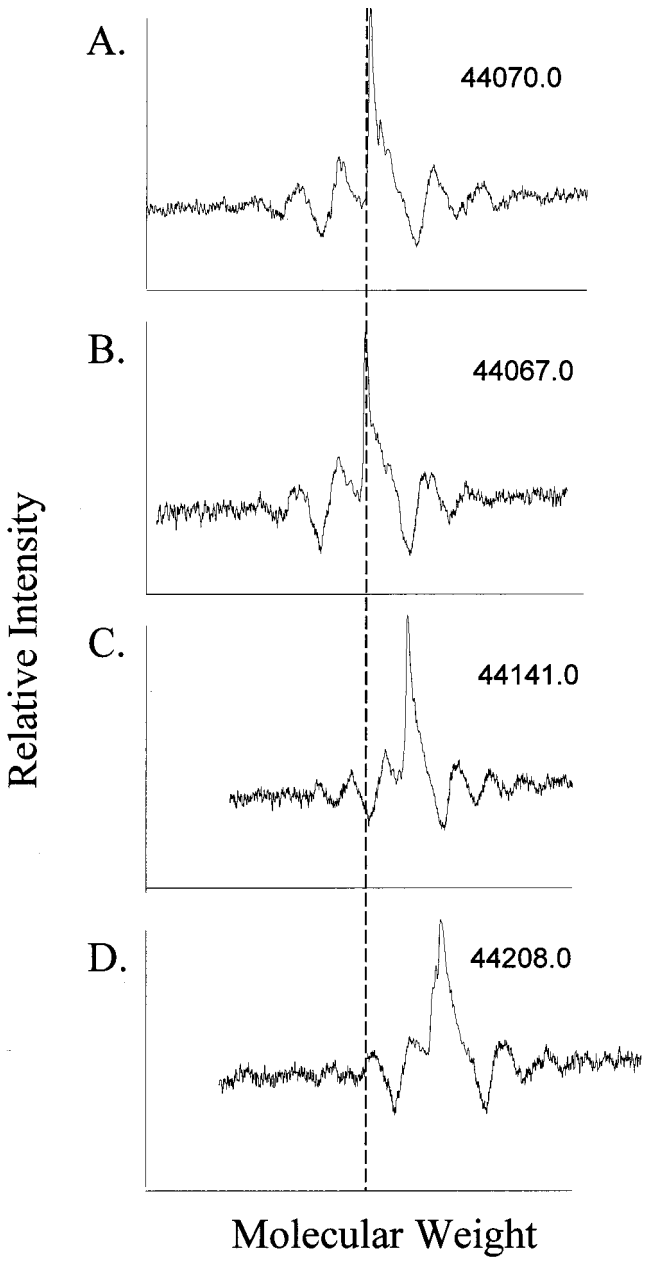

FIGURE 2: Mass spectrometric analysis of MKK-activated JNK3α1. Approximately 5 pmol (227 ng) of JNK3α1 was characterized by LC−MS. (A) Mass spectrum of untreated JNK3α1. (B) Mass spectrum of MKK4-treated JNK3α1. (C) Mass spectrum of MKK7-activated JNK3α1. (D) Mass spectrum of MKK4 + MKK7-activated JNK3α1.

consistent with a single phosphorylation and two oxidations (Figure 2C). The 3 Da difference from the expected mass is within experimental detection limits. Finally, MKK4 + MKK7-activated JNK3α1 had a MW of 44 208 Da consistent with bisphosphorylation and one oxidation (Figure 2D), indicating stoichiometric conversion to the bisphosphorylated form and accounting for the expected mass changes within the detection limits. Moreover, we were able to determine the location of the phosphorylation sites by digesting the bisphosphorylated JNK3α1 with porcine trypsin and analyzing the resultant peptide fragments with cHPLC−MS/MS. Approximately 73% of the complete amino acid sequence for JNK3α1 was revealed by this analysis. The only peptide found to be phosphorylated had the sequence TAGTSFMMT-(PO_3)PY(PO_3)VVTR, where the phosphorylation sites are

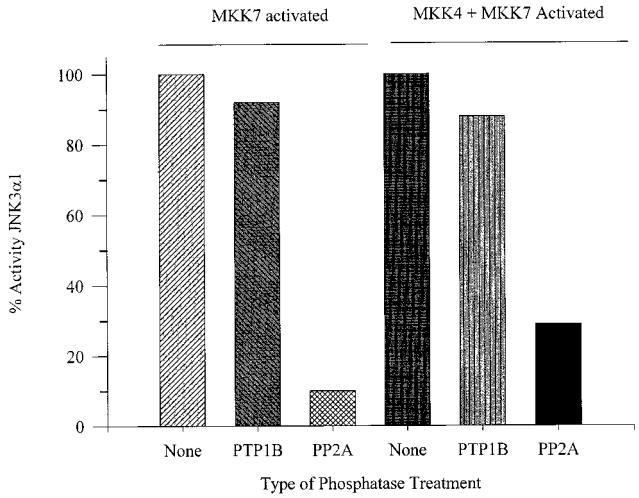

FIGURE 3: Percent activity of MKK7-activated JNK3α1 or MKK4 + MKK7-activated JNK3α1 before and after phosphatase treatment. JNK3α1 activated in vitro with MKK7 (three bar graphs on the left) or MKK4 + MKK7 (three bar graphs on the right) was assayed for its kinase activity toward GST-ATF2 after either no treatment or treatment for 15 min at 30 °C with either 180 nM PTP1B or 200 nM PP2A. Phosphatase reactions were terminated with 5 mM Na_3VO_4 for PTP1B or 10 μg/mL okadaic acid for PP2A, and JNK3α1 kinase activity was measured as described in the Materials and Methods.

indicated. It should be noted that this peptide contained the sequence to which the anti-phospho-JNK antibody was generated.

Dephosphorylation of JNK3α1. Figure 3 presents the JNK3α1 kinase activity remaining after MKK7 or MKK4 + MKK7-activated samples were treated with either PTP1B or PP2A. Treatment of MKK7-activated JNK3α1 with the tyrosine phosphatase, PTP1B, does not affect JNK3α1 activity whereas treatment with the serine/threonine phosphatase, PP2A, reduces JNK3α1 activity by 90%. Similarly, PTP1B treatment does not affect MKK4 + MKK7-activated JNK3α1 activity, but PP2A treatment reduces the activity by 70%. Anti-phosphotyrosine Western analysis of PTP1B-treated samples showed a marked decrease in phosphotyrosine immunoreactivity, indicating that PTP1B was indeed active (data not shown).

Steady-State Kinetics. Comparison of the maximal velocity, V_{max}, measured at the steady state for the conversion of GST-ATF2 to phosphorylated GST-ATF2 for the various MKK-activated or unactivated forms of JNK3α1 is given in Figure 4. V_{max} for nontreated and MKK4-activated JNK3α1 was 0.2 nM/min and is considered the basal, or nonactivated, specific activity of JNK3α1. MKK7-activated and MKK4 + MKK7-activated JNK3α1 had V_{max} 250-fold and 715-fold greater than nontreated JNK3α1, respectively (Figure 4).

The steady-state rate constants for the phosphorylation of GST-ATF2 catalyzed by MKK7-activated and MKK4 + MKK7-activated JNK3α1 along with the IC_{50} value for SB203580 are presented in Table 1. The turnover number, k_{cat}, and the K_m values for ATP and GST-ATF2 were found to be within 2-fold between those of MKK7-activated JNK3α1 and MKK4 + MKK7-activated JNK3α1. SB203580 was a more potent inhibitor of MKK7-activated JNK3α1 by approximately 4-fold compared to MKK4 + MKK7-activated JNK3α1.

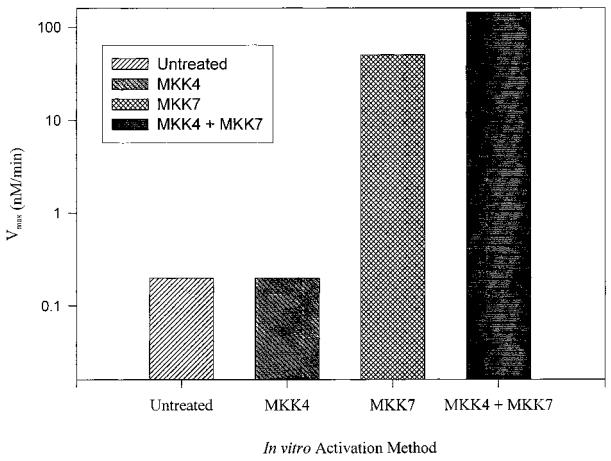

FIGURE 4: In vitro activation of JNK3α1. The kinase activity of JNK3α1 was measured after treatment for 2 h at 30 °C by 100 nM MKK4, 100 nM MKK7, or 100 nM MKK4 + 100 nM MKK7 or no treatment. JNK3α1 kinase activity (nM/min) was measured as described in the Materials and Methods.

Table 1: Steady-State Rate Constants and IC_{50} Determination for the Phosphorylation of GST-ATF2 Catalyzed by JNK3α1 Activated by MKK7 or MKK4 + MKK7[a]

activator	$K_{m(GST-ATF2)}$ (μM)	$K_{m(ATP)}$ (μM)	k_{cat} (min^{-1})	$IC_{50(SB203580)}$ (nM)
MKK7	0.7 ± 0.3	4.3 ± 1.7	2.6 ± 0.4	200 ± 40
MKK4 + MKK7	0.4 ± 0.1	1.9 ± 0.5	5.3 ± 0.6	790 ± 150

[a] The kinetic parameters were calculated from the equation for a ternary complex (*20*). The errors shown are standard errors. Data are from the average of two experiments each filtered in triplicate for the steady-state rate constants and the average of three experiments each filtered in triplicate for the IC_{50} determination.

DISCUSSION

Phosphorylation of JNK3α1. To quantitatively understand the contributions MKK4 and MKK7 make to in vitro activation of JNK3α1, we studied the phosphorylation and subsequent enzyme activation of JNK3α1 utilizing steady-state kinetics and mass spectrometry. To date there are neither reports on how JNK3 is activated nor any kinetic characterization of a putative in vivo substrate, ATF2. Rather, many studies addressing the issue of JNK activation have used immunoprecipitation of JNK1, MKK4, and MKK7 or co-expression to assess the phosphorylation and activation of JNK1 (*15*−*17*). Other reports utilizing purified JNK1 pathway components have largely analyzed JNK phosphorylation by SDS−PAGE analysis and autoradiography (*21*, *22*). Thus, assessment of JNK3α1 activation and kinase activity by mass spectrometry and kinetic analysis should help elucidate the JNK3α1 activation pathway and compare and contrast JNK3α1 activation to JNK1, p38, and ERK2 activation.

We chose in vitro activation of JNK3α1 for several reasons. First, most MAP kinases are easily expressed in *E. coli* (*13*, *23*−*25*) yet have very little basal kinase activity unless coexpressed with upstream activators or activated in vitro by MAP kinase kinases. Moreover, unlike p38 which can be expressed in S2 *Drosophila* cells and isolated fully active (*19*, *27*), JNK3α1 cannot be fully activated when expressed in *Sf*-9 cells (LoGrasso et al., unpublished results). Most importantly, however, is that in vitro activation of

JNK3α1 by purified JNK pathway components allows for a systematic and quantitative assessment of the individual and collective contributions MKK4 and MKK7 make toward JNK3α1 activation, thus allowing potential extrapolation of their roles in vivo.

The combination of Western analysis and mass spectrometry (Figures 1 and 2) allowed us to evaluate the phosphorylation state of JNK3α1 after various activation conditions. Our results concerning MKK4- and MKK7-treated JNK3α1 were consistent with those of Lawler et al. (*18*) who demonstrated using phosphoamino acid analysis of tryptic digests that MKK4 + MKK7-activated JNK1 was bisphosphorylated, with one phosphorylation on tyrosine and one on threonine. Collectively, the two phosphorylations seen by mass spectrometry, MS/MS analysis of tryptic digests showing only Thr 221 and Tyr 223 phosphorylated, and an anti-phospho-JNK specific antibody that only recognizes bisphospho-Thr 221 and -Tyr 223 is strong evidence for only two phosphorylations, both occurring in the phosphorylation loop and not elsewhere in the protein. Furthermore, the 2-fold increase in k_{cat} seen in the MKK4 + MMK7-treated sample was due to Tyr 223 phosphorylation and not additional Thr phosphorylation evidenced by the increase in Tyr immunoreactivity seen by Western analysis (Figures 1b,c) upon treatment with MKK4 in addition to MKK7. Moreover, there was a larger change (~4-fold) in the specificity constant, k_{cat}/K_m, for the bisphosphorylated sample, indicating the contribution of Tyr phosphorylation to the overall specificity. Finally, it is highly unlikely that there were any spurious phosphorylations outside the activation loop as seen by Lawler et al. (*18*) especially since the additional phosphorylation they observed was unique to the fusion protein they used. Since our JNK3α1 did not contain the His (*6*) fusion, this spurious phosphorylation can be categorically ruled out.

The bisphosphorylation of JNK3α1 after MKK4 + MKK7 activation suggests that, like JNK1, JNK3α1 needs both MKK4 and MKK7 to be fully phosphorylated in the activation loop. Moreover, it is likely that MKK7 is responsible for threonine phosphorylation, and once JNK3α1 is threonine phosphorylated, then MKK4 can phosphorylate JNK3α1 on tyrosine. It is difficult to quantitatively compare the activity of MKK4 + MKK7-activated JNK3α1 in our study to that of MKK4 + MKK7-activated JNK from Lawler et al. (*18*) due to the different reaction conditions used. For example, our experimental conditions for JNK3α1 activity were under initial velocity conditions such that less than 10% conversion of GST-ATF2 occurred during the entire reaction and utilized 2 nM JNK3α1 compared to 200 nM JNK1 in Lawler et al. (*18*). Qualitatively, however, MKK4 + MKK7 activation gave maximal activity of both JNK3α1 and JNK1 compared to activation of JNK by either single MAP kinase kinase.

It should be noted that the 250-fold difference in activity we saw between MKK7-activated JNK3α1 and MKK4-treated JNK3α1 is different from that seen for JNK1 activated by MKK4 or MKK7 (*18*). Since the magnitude of the MKK4 or MKK7 JNK1 activation over basal activity described by Lawler et al. (*18*) is unknown, it is difficult to specifically address the differences seen in MKK4 treatment of JNK3α1 compared to JNK1 except to say that perhaps JNK1 is a better substrate than JNK3α1 for MKK4. Our results for MKK4-treated JNK3α1 are however similar to those of Derijard et al. (*21*) in that in their MKK4 activation studies of JNK1 they saw a faint JNK1 phosphorylation as detected by autoradiography. This faint signal despite the high specific activity [^{32}P]ATP used in the reaction suggests low-level phosphorylation of JNK1 and is similar to the low-level tyrosine phosphorylation we see with anti-phosphotyrosine detection (Figure 1B). However, the activation of JNK3α1 by MKK7 to nearly 30% of maximal activity may be unique to JNK3α1 compared to JNK1, p38, or ERK2 in that, unlike these other MAP kinases, JNK3α1 may only need threonine phosphorylation for near maximal activity. The fact that the turnover number for MKK7-activated JNK3α1 is 2−3-fold less than that for MKK4 + MKK7-activated JNK3α1, coupled with our observation that PTP1B does not significantly reduce the activity of MKK4 + MKK7-activated JNK3α1 (Figure 3) compared to PP2A, which reduces this activity by 70%, strongly suggests that Thr phosphorylation of JNK3α1 may be the primary requirement for activity. This observation is different from that seen for p38 (*23*, *27*) and ERK2 (*28*) and may make JNK3α1 a unique member of the MAP kinase family with regard to activation requirements.

Finally, there are several studies utilizing immunoprecipitates showing that MKK7 and MKK4 are individually responsible for JNK1 activation (*15*−*17*). Since all of these studies rely on immunoprecipitation of either MKK4 or MKK7, one cannot be certain that the observed effects are due solely to MKK4 or MKK7 since it is likely that other signal transduction proteins are being coprecipitated. Indeed, there are many such examples of immunoprecipitated complexes that are composed of multiple components (*29*−*31*). Thus, it is possible that MKK7 may be associated with MKK4 immunoprecipitates, or MKK4 with MKK7 immunoprecipitates, further complicating the interpretation of the individual roles for each MKK.

Functional Consequences of Tyrosine and Threonine Phosphorylation. The kinetic analysis in this study for the regulation of JNK3α1 activity and substrate binding is consistent with the structural data for JNK3α1 and the related MAP kinase, ERK2. Our results are consistent with a model where the nonphosphorylated form of JNK3α1 has minimal activity possibly due to tyrosine 223 blocking part of the substrate binding domain (*13*). Upon threonine 221 phosphorylation, JNK3α1 becomes active (Figure 4) likely because of a large conformational change in the phosphorylation lip that may remove Tyr 223 from the substrate binding channel. In addition, once Tyr 223 is repositioned, it is able to be phosphorylated by MKK4. Since Tyr 223 has already been removed from the substrate binding channel prior to Tyr phosphorylation (i.e., during Thr 221 phosphorylation), no additional increase in substrate binding is seen upon Tyr 223 phosphorylation (Table 1). This phosphorylation lip movement and unblocking of the substrate binding channel suggested by our kinetic data are consistent with domain movements hypothesized by comparison of the crystal structures of unphosphorylated JNK3α1 and bisphosphorylated ERK2 (*13*, *28*). Moreover, the observation for JNK3α1 being phosphorylated in a processive manner with Thr 221 being phosphorylated before Tyr 223 is consistent with the results seen by Lawler et al. (*18*) for JNK1.

Finally, the K_m values for GST-ATF2 and ATP were within 2-fold for the Thr 221 monophosphorylated JNK3α1 and the Thr 221/Tyr 223 bisphosphorylated JNK3α1, indicating that phosphorylation of Tyr 223 has little effect on both ATF2 and ATP binding. Moreover, since no change is seen in the $K_{m(ATF2)}$ after Tyr 223 phosphorylation, it is likely that Thr 221 phosphorylation occurs first with concomitant removal of Tyr 223 from the substrate binding domain. The $K_{m(ATP)}$ for MKK4 + MKK7-activated JNK3α1 was 1.9 μM, the same as the $K_{m(ATP)}$ reported by Anderson (*32*) for JNK2, suggesting JNK3α1 and JNK2 have the same binding affinities for ATP.

In addition to having the same binding affinities for ATP, JNK3α1 and JNK2α1 also have similar binding affinities for SB203580. The IC_{50} for SB203580 for JNK3α1 is 790 ± 150 nM and compares favorably to that determined for JNK2α1 (290 ± 110 nM), which was measured under similar conditions (*33*). SB203580 is an ATP-competitive inhibitor of p38 MAP kinase (*26*, *34*) and is likely to be ATP-competitive for JNK as well. However, several reports indicate that SB203580 is not an inhibitor of JNK1 (*35*, *36*). Since the $K_{m(ATP)}$ has not been reported, it is difficult to say whether this is the reason for the differences in the observed IC_{50} between JNK1 and JNKs 2 and 3. If the JNK1 $K_{m(ATP)}$ is similar to those of JNK3α1 and JNK2α1, the lack of inhibition for JNK1 up to 10 μM SB203580 seen by Gum et al. (*35*) can most likely be attributed to the inhibition experimental conditions having the ATP concentration at 50 μM. This would shift the IC_{50} such that at 10 μM SB-203580 there appears to be no inhibition.

The experiments we describe are unique in that they utilized purified components of the JNK3α1 signaling pathway to assess the ability of MKK4, MKK7, and the combination of MKK4 + MKK7 to phosphorylate and activate JNK3α1. Our results suggest a processive mechanism for JNK3α1 activation that requires phosphorylation of Thr 221 by MKK7 prior to phosphorylation of Tyr 223 by MKK4. Only when JNK3α1 was activated by both upstream MAP kinase kinases was it fully phosphorylated. Moreover, catalysis and binding of substrates and inhibitor were not greatly affected by phosphorylation of tyrosine, but rather by the placement of tyrosine in the substrate binding domain, which in turn is likely controlled by the phosphorylation state of Thr 221. Indeed, JNK3α1 may be unique among the MAP kinase family members in that phosphorylation on Thr 221 in the active site may be sufficient for JNK3α1 activation, with additional Tyr 223 phosphorylation increasing activity only 3-fold. It is interesting to speculate that what we see in vitro may also be true in vivo and may be the mechanism by which JNK3α1 is regulated.

ACKNOWLEDGMENT

We are grateful to Dr. Alice Marcy for critical review of this manuscript and to Doug Wisniewski for help with the illustrations.

REFERENCES

1. Ip, Y. T., and Davis, R. J. (1998) *Curr. Opin. Cell Biol. 10*, 205−219.
2. Minden, A., and Karin, M. (1997) *Biochim. Biophys. Acta 1333*, F85−F104.
3. Yang, D. D., Kuan, C.-Y., Whitmarsh, A. J., Rincon, M., Zheng, T. S., Davis, R. J., Rakic, P., and Flavell, R. A. (1997) *Nature 389*, 865−870.
4. Hibi, M., Lin, A., Smeal, T., Minden, A., and Karin, M. (1993) *Genes Dev. 7*, 2135−2148.
5. Derijard, B., Hibi, M., Wu, I.-H., Barrett, T., Su, B., Deng, T., Karin, M., and Davis, R. J. (1994) *Cell 76*, 1025−1037.
6. Gupta, S., Barrett, T., Whitmarsh, A. J., Cavanagh, J., Sluss, H. K., Derijard, B., and Davis, R. J. (1996) *EMBO J. 15*, 2760−2770.
7. Livingstone, C., Patel, G., and Jones, N. (1995) *EMBO J. 14*, 1785−1797.
8. Hu, M. C−T., Qiu, W. R., and Wang, Y.-P. (1997) *Oncogene 15*, 2277−2287.
9. Zhang, Y., Zhou, L., and Miller, C. A. (1998) *Proc. Natl. Acad. Sci. U.S.A. 95*, 2586−2591.
10. Mohit, A. A., Martin, J. H., and Miller, C. A. (1995) *Neuron 14*, 67−78.
11. Xia, Z., Dickens, M., Raingaued, J., Davis, R. J., and Greenberg, M. E. (1995) *Science 270*, 1326−1331.
12. Maroney, A. C., Glicksman, M. A., Basma, A. N., Walton, K. M., Knight, E., Jr., Murphy, C. A., Bartlett, B. A., Finn, J. P., Angeles, T., Matsuda, Y., Neff, N. T., and Dionne, C. A. (1998) *J. Neurosci. 18*, 104−111.
13. Xie, X., Gu, Y., Fox, T., Coll, J. T., Fleming, M. A., Markland, W., Caron, P. R., Wilson, K. P., and Su, M. S.−S. (1998) *Structure 6*, 983−991.
14. Yang, D., Tournier, C., Wysk, M., Lu, H.-T., Xu, J., Davis, R. J., and Flavell, R. A. (1997) *Proc. Natl. Acad. Sci. U.S.A. 94*, 3004−3009.
15. Deacon, K., and Blank, J. L. (1997) *J. Biol. Chem. 272*, 14489−14496.
16. Lu, X., Nemoto, S., and Lin, A. (1997) *J. Biol. Chem. 272*, 24751−24754.
17. Holland, P. M., Suzanne, M., Campbell, J. S., Noselli, S., and Cooper, J. A. (1997) *J. Biol. Chem. 272*, 24994−24998.
18. Lawler, S., Fleming, Y., Goedert, M., and Cohen, P. (1998) *Curr. Biol. 8*, 1387−1390.
19. LoGrasso, P. V., Frantz, B., Rolando, A. M., O'Keefe, S. J., Hermes, J. D., and O'Neill, E. A. (1997) *Biochemistry 36*, 10422−10427.
20. Leatherbarrow, R. J. (1992) *GraFit*, version 3.0, Erithacus Software Ltd., Staines, U.K.
21. Derijard, B., Raingeaud, J., Barrett, T., Wu, I.-H., Han, J., Ulevitch, R. J., and Davis, R. J. (1995) *Science 267*, 682−685.
22. Tournier, C., Whitmarsh, A. J., Cavanagh, J., Barrett, T., and Davis, R. J. (1997) *Proc. Natl. Acad. Sci. U.S.A. 94*, 7337−7342.
23. Raingeaud, J., Gupta, S., Rogers, J. S., Dickens, M., Han, J., Ulevitch, R. J., and Davis, R. J. (1995) *J. Biol. Chem. 270*, 7420−7426.
24. Jiang, Y., Chen, C., Li, Z., Guo, W., Gegner, J. A., Lin, S., and Han, J. (1996) *J. Biol. Chem. 271*, 17920−17926.
25. Khokhlatchev, A., Xu, S., English, J., Wu, P., Schaefer, E., and Cobb, M. H. (1997) *J. Biol. Chem. 272*, 11057−11062.
26. Lisnock, J. M., Tebben, A., Frantz, B., O'Neill, E. A., Croft, G., O'Keefe, S. J., Li, B., Hacker, C., de Laszlo, S., Smith, A., Libby, B., Liverton, N., Hermes, J., and LoGrasso, P. (1998) *Biochemistry 37*, 16573−16581.
27. Frantz, B., Klatt, T., Pang, M., Parsons, J., Rolando, A., Williams, H., Tocci, M. J., O'Keefe, S. J., and O'Neill, E. A. (1998) *Biochemistry 37*, 13846−13853.
28. Canagarajah, B., Khokhlatchev, A., Cobb, M., and Goldsmith, E. J. (1997) *Cell 90*, 859−869.
29. DiDonato, J. A., Hayakawa, M., Rothwarf, D. M., Zandi, E., and Karin, M. (1997) *Nature 388*, 548−554.
30. Mercurio, F., Zhu, H., Murray, B. W., Shevchenko, A., Bennett, B. L., Li, J. W., Young, D. B., Barbosa, M., Mann, M., Manning, A., and Rao, A. (1997) *Science 278*, 860−866.

31. Whitmarsh, A. J., and Davis, R. J. (1998) *TIBS 23*, 481−485.
32. Anderson, D. (1997) The National Health Care Congress: Cell Signaling, San Diego, CA, July 9−11, 1997.
33. Liverton, N., Buthcher, J. W., Claiborne, C. F., Claremon, D. A., Libby, B. E., Nguyen, K. T., Pitzenberger, S. M., Selnick, H. G., Smith, G. R., Tebben, A., Vacca, J. P., Varga, S. L., Agarwal, L., Dancheck, K., Forsyth, A. J., Fletcher, D. S., Frantz, B., Hanlon, W. A., Harper, C. F., Hofsess, S. J., Kostura, M., Lin, J., Luell, S., O'Neill, E. A., Orevillo, C. J., Pang, M., Parsons, J., Rolando, A., Sahly, Y., Visco, D., and O'Keefe, S. J. (1999) *J. Med. Chem. 42*, 2180−2190.
34. Young, P. R., McLaughlin, M. M., Kumar, S., Kassis, S., Doyle, M. L., McNulty, D., Gallagher, T. F., Fisher, S., McDonnell, P. C., Carr, S. A., Huddleston, M. J., Seibel, G., Porter, T. G., Livi, G. P., Adams, J. L., and Lee, J. C. (1997) *J. Biol. Chem. 272*, 12116−12121.
35. Gum., R. J., McLaughlin, M. M., Kumar, S., Wang, Z., Bower, M. J., Lee, J. C., Adams, J. L., Livi, G. P., Goldsmith, E. J., and Young, P. R. (1998) *J. Biol. Chem. 273*, 15605−15610.
36. Clerk, A., and Sugden, P. H. (1998) *FEBS Lett. 426*, 93−96.

BI992410+